Biogeosciences
Discussions

Open Access

EGU

Mapping the reduction in carbon uptake in subarctic birch forests due to insect outbreaks

Per-Ola Olsson, Michal Heliasz, Hongxiao Jin, Lars Eklundh

Department of Physical Geography and Ecosystem Science, Lund University, Sölvegatan 12, S-223 62 Lund, Sweden.

5   *Correspondence to*: Per-Ola Olsson (per-ola.olsson@nateko.lu.se)

Abstract. It is projected that forest disturbances, such as insect outbreaks, will have an increasingly negative impact on forests with a warmer climate. These disturbance events can have a substantial impact on forests' ability to absorb atmospheric CO_2, and may even turn forests from carbon sinks into carbon sources; hence, it is important to develop methods to both monitor forest disturbances and to quantify the impact of these disturbance events on the carbon balance. In

10   this study we present a method to monitor insect induced defoliation in a subarctic birch forest in northern Sweden, and to quantify the impact of these outbreaks on gross primary productivity (GPP). Since frequent cloud cover in the study area requires data with high temporal resolution and limits the use of finer spatial resolution sensors such as Landsat, defoliation was mapped with remote sensing data from the MODIS sensor with 250×250 m spatial resolution. The impact on GPP was estimated with a light use efficiency (LUE) model that was calibrated with GPP data obtained from eddy covariance (EC)

15   measurements for years with undisturbed birch forest and for years with insect induced defoliation. Two methods were applied to estimate the impact on GPP: (1) A GPP reduction factor derived from EC-measured GPP was applied to estimate GPP loss, and (2) a LUE model was run both for undisturbed and defoliated forest and the differences in modelled GPP were derived. In the study area of 100 km^2 the results showed a total decrease in carbon uptake over three outbreak years 2004, 2012, and 2013 of 44.6 ±13 Gg C, which is of the same magnitude as the estimated annual GPP of 41.1 ±12 Gg C for a year

20   without disturbance. In the most severe outbreak year (2012), 76% of the birch forests were defoliated and annual GPP was merely 50% of GPP for years without disturbances. The study has generated valuable data that improve previous studies on impact estimates and demonstrates a potential for mapping insect disturbance impact over extended areas.

Keywords: Insect defoliation, subarctic mountain birch, MODIS, GPP, LUE

1 Introduction

25   It is estimated that forests account for half of the global terrestrial net primary productivity and act as important sinks of atmospheric CO_2 (Bonan 2008). Forests in the northern hemisphere contribute significantly to this sink, with the mid- and high latitude ecosystems as major contributors (Goodale et al. 2002; Kurz et al. 2008b). The high latitude forests are, however, predicted to be among the ecosystems that are most strongly influenced by climate change (Kurz et al. 2008b); a

warmer climate is likely to increase forest productivity, and result in higher uptake of CO_2 from the atmosphere. On the other hand, it is projected that the impact of forest disturbances will increase with a warmer climate (Seidl et al. 2014), and there are indications that disturbances such as wind, fires, and insect outbreaks have lead to saturation of the carbon sinks in European forests (Nabuurs et al. 2013). One important forest disturbance agent is insects; it is projected that the temporal and spatial dynamics, as well as the intensities and ranges of insect herbivore outbreaks will be influenced by global warming (Vanhanen et al. 2007; Battisti 2008; Jepsen et al. 2008; Netherer & Schopf 2010). These insect outbreaks can severly disturb forest ecosystems and have a strong impact on carbon dynamics (Kurz et al. 2008a; Jepsen et al. 2009; Heliasz et al. 2011). Quantitative effects of insect outbreaks on the carbon balance are, however, not well known (Clark et al. 2010; Schäfer et al. 2010; Hicke et al. 2012), and insect outbreaks are generally excluded in large scale carbon modelling, which may result in overestimation of forests' ability to act as carbon sinks (Kurz et al. 2008b; Hicke et al. 2012). Consequently, it is important to develop methods both to monitor the spatial extent of insect outbreaks and to quantify the impact of these outbreaks on the carbon balance.

One alternative to estimate the impact on forest productivity is modelling: The impact of a large-scale outbreak of the mountain pine beetle (*Dendroctonus ponderosae* Hopkins) in British Columbia, Canada, was studied with a forest ecosystem model by Kurz et al. (2008a). The impact on the carbon balance of gypsy moth (*Lymantria dispar* L.) defoliation in New Jersey, USA, was modelled with both a canopy assimilation model (Schäfer et al. 2010) and a terrestrial biosphere model (Medvigy et al. 2012). Dymond et al. (2010) modelled the impact of Spruce Budworm (*Choristoneura fumiferana* Clem.) outbreaks in eastern Canada, and Landry et al. (2016) developed a Marauding Insect Module (MIM) in the Integrated Biosphere Simulator (IBIS) that enables simulation of insect outbreak for three different insect functional types. Another alternative to quantify the influence of an insect outbreak on the carbon balance is to apply eddy covariance (EC) measurements: Brown et al. (2010) studied how a mountain pine beetle outbreak influenced net ecosystem productivity (NEP) in British Columbia, Canada; Clark et al. (2010, 2014) studied difference in NEE between undisturbed years and years with severe defoliation by the gypsy moth in New Jersey, USA; and Heliasz et al. (2011) estimated the reduction in net ecosystem exchange (NEE) during the growing season due to an autumnal moth (*Epirrita autumnata* Borkhausen) and winter moth (*Operophtera brumata* L.) outbreak in northern Sweden in 2004. Even though not explicitly studied, there was also gypsy moth defoliation present in a time-series of EC-measurement in southern France (Allard et al. 2008). These methods generate valuable data on the impact of insect defoliation on the carbon balance; however, to quantify the total regional impact, data on the extent of defoliation events are required.

To generate wall-to-wall estimates of the disturbance effect on the carbon balance, remotely sensed data from satellites can be used. Several studies have demonstrated that satellite based remote sensing techniques can be applied to detect insect disturbances with high accuracy; see e.g. Wulder et al (2006); Adelabu et al. (2012) and Rullan-Silva et al. (2013) for reviews. In this paper we study outbreaks of autumnal moth and winter moth in subarctic mountain birch (*Betula pubescens ssp. Czerepanovii* N.I. Orlova) forests in northern Sweden. These outbreaks are often followed by within-season recovery of the foliage in parts of the outbreak areas, which in combination with cloudy conditions can limit the possibility to map the

outbreaks with remote sensing methods. Nevertheless, outbreaks of autumnal and winter moth have been mapped in northern Fennoscandia with high accuracy with Landsat data (Tømmervik et al. 2001; Babst et al. 2010). The low temporal resolution of Landsat can, however, be a limitation; as an example, only fractions of the area included in this study were visible in Landsat data during the peak of a severe outbreak in 2013. An alternative to Landsat data is to utilize coarse spatial

5   resolution data from e.g. the moderate resolution imaging spectroradiometer (MODIS) sensor, which provides data with high (daily) temporal resolution and a spatial resolution of 250×250 m or coarser. MODIS derived Normalized Difference Vegetation Index (NDVI) have been used to map autumnal and winter moth outbreaks with high accuracy in northern Fennoscandia (Jepsen et al. 2009); and Olsson et al. (2016) developed a method for near real-time monitoring of insect induced defoliation that also facilitates monitoring of refoliation later in the growing season.

10   Furthermore, there is a large body of research demonstrating that vegetation primary productivity can be estimated with remotely sensed data and a light use efficiency (LUE) approach (e.g. Prince 1991; Ruimy et al. 1994; Running et al. 2004; Xiao et al. 2004; Wu et al. 2010; McCallum et al. 2013; Gamon 2015). The LUE concept was introduced by Monteith (1972, 1977), suggesting that the primary productivity of plants has a strong linear relationship to the absorbed amount of photosynthetically active radiation (APAR), i.e. solar radiation in the spectral range 400–700 nm that is absorbed by the

15   plant canopy. Since near-linear relationships between satellite derived vegetation indices and the fraction absorbed PAR (fAPAR) have been established (e.g. Asrar et al. 1984; Sellers 1987; Goward & Huemmrich 1992; Myneni & Williams 1994; Olofsson and Eklundh 2007), it is possible to create a LUE model on the form (Prince 1991; Running et al. 2004):

$$GPP = \varepsilon \times fAPAR \times PAR$$

where *GPP* is gross primary productivity, ε is the light use efficiency coefficient and *fAPAR* is estimated as:
20   $fAPAR = a + b \times NDVI$ (Myneni & Williams 1994). The light use efficiency coefficient varies between vegetation types and variability in meteorology, hence, it is common to model ε with a maximum efficiency depending on vegetation type, and reduction factors based on temperature and vapour pressure deficit (e.g. Field et al. 1995; Prince & Goward 1995; Potter et al. 1999; Turner et al. 2003). In cold climates, temperature is the main limiting factor for photosynthetic capacity (Bergh et al. 1998), and it has been shown that the variability in ε can be modelled with temperature data only (Lagergren et al. 2005).

25   For ecosystems dominated by non-vascular plants it should, however, be noted that water stress is a major limiting factor (Liljedahl et al. 2011). This type of LUE model could be suitable for large-area estimates of the impact of forest disturbance on the uptake component of the carbon balance, GPP. However, to the knowledge of the authors, no previous study has utilized remote sensing data and a LUE model to monitor and quantify the impact of an insect outbreak on carbon uptake.

In this study we utilized EC-measured GPP to develop a LUE model, and satellite based remote sensing data to map insect
30   induced defoliation, as well as to upscale the impact on GPP of this defoliation with the aid of the LUE model. This combination of EC-data to calibrate a LUE model, and remote sensing data to map and quantify the impact of insect disturbances on the carbon balance is a major advantage compared to methods that lack spatial observations. The method was developed in insect-defoliated subarctic mountain birch forests in northern Sweden. The fractional absorbed

photosynthetically active radiation was derived from NDVI obtained from the MODIS sensor with a temporal resolution of eight days. Temperature data, used to model variability in ε, and PAR was obtained from an EC-tower. Our main study objective was to quantify the reduction in GPP due to insect defoliation in the birch forest of a subarctic valley of northern Sweden between 2000 and 2015, a period during which three significant insect outbreak events have occurred. The analysis

5   was achieved with two methods: (1) finding GPP for undisturbed forest and estimate the impact of an insect outbreak with a common reduction factor derived from EC-data; and (2) by applying a LUE model for both undisturbed and defoliated pixels and computing the differences.

2 Materials and methods

2.1 Study area

10   The study area was the mountain birch (*Betula pubescens ssp. Czerepanovii* N.I. Orlova) forests in a valley south-west of Abisko village (68.35N, 18.82E), and along the lake Torneträsk, as illustrated in Fig. 1 (green). The area is located in the subarctic zone in northern Sweden with lake Torneträsk at an altitude of 345 m.a.s.l. and with the highest mountains reaching 1 700 m.a.s.l. (Interact, 2016). These birch forests are infested by the autumnal moth (*Epirrita autumnata* Borkhausen) and the winter moth (*Operophtera brumata* L.) in time intervals of 9–10 years (Bylund 1995; Tenow et al.

15   2007). The first reported outbreaks by the autumnal moth in northern Fennoscandia are from mid-1800, and the winter moth has been reported in the northern parts of Fennoscandia since late 1800 (Tenow 1972). These insect outbreaks strongly influence the birch forests (Ammunét et al. 2015); severe defoliation events may result in stem mortality, requiring decades of recovery (e.g. Tenow 1996; Tenow & Bylund 2000; Jepsen et al. 2013), and understorey vegetation can shift into more grass dominated communities (Karlsen et al. 2013; Jepsen et al. 2013). Root-associated fungal communities can change

20   (Saravesi et al. 2015) as well as chemical and physical properties of the soil (Kaukonen et al. 2013). A warmer climate, especially a lower frequency of years with extremely cold winters, as reported by Callaghan et al. (2010), strongly influences birch moth populations (Babst et al. 2010). The autumnal moth outbreaks have expanded into colder, more continental regions, and the winter moth has reached further to the north-east into areas where the autumnal moth previously dominated (Jepsen et al. 2008). The latest outbreaks occurred in 2004, with a documented reduction in carbon uptake of 89% at an EC

25   tower (Heliasz et al. 2011), and in 2012 and 2013 (Bengt Landström, County administrative board of Norrbotten, pers. comm. 31.10.2013). These outbreak events were included in this study.
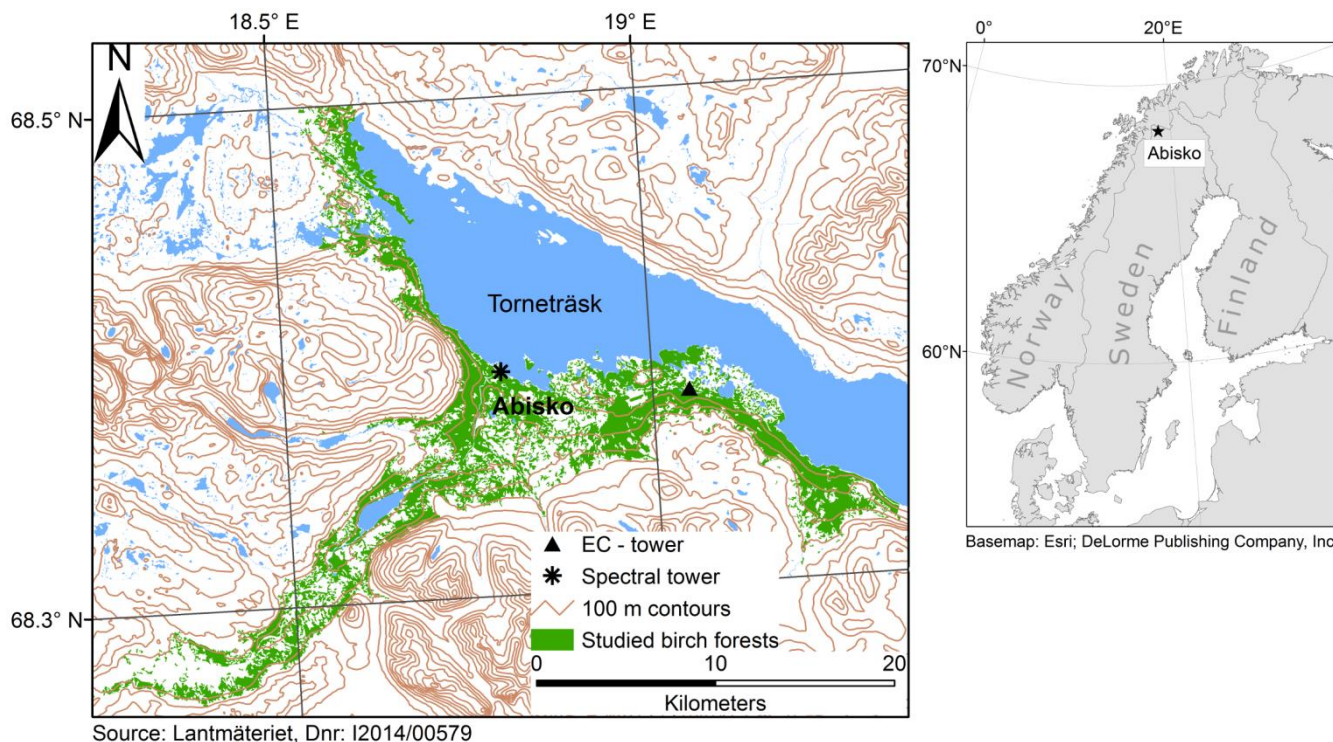
Figure 1. The studied birch forest (green) along the south-west part of lake Torneträsk and in the valley to the south-west of Abisko village. The locations of the eddy covariance (EC) tower used to obtain GPP, and the spectral tower used to obtain fAPAR data are also shown. Reference system is SWEREF99 TM and latitude and longitude are in WGS84. Source of background map: Lantmäteriet (Dnr: I2014/00579).

2.2 Data

2.2.1 Remote sensing data and smoothing of time-series

We used two Terra/MODIS satellite data products with eight days temporal resolution: (1) MOD09Q1 version 5, surface reflectance in the red and near infrared (NIR) bands, including quality assurance (QA) information, with 250×250 m spatial resolution, used mainly to derived NDVI (LPDAAC 2016a); and (2) MOD09A1 version 5, surface reflectance, as well as QA data, with 500×500 m spatial resolution (LPDAAC 2016b), utilized due to the product's more comprehensive QA data. NDVI was computed from the MODIS data as (Rouse et al. 1973; Tucker 1979):

$$NDVI = (NIR\text{-}red)/(NIR\text{+}red) \tag{1}$$

where *red* is reflectance in the red wavelength band, and *NIR* is reflectance in the near infrared wavelength band. We created time-series for the period 2000–2014 and for all pixels in the study area and processed in TIMESAT ver. 3.2. TIMESAT is a software package used to reduce the influence of noise by fitting smoothed functions to time-series of data (Jönsson & Eklundh 2002, 2004). In this study we applied the same fittings and weights as in Olsson et al. (2016): Double logistic functions were used to smooth the data and the NDVI observations were classified into quality classes based on QA data

from both MOD09Q1 and the more comprehensive QA-flags in MOD09A1. In this study we use the term $NDVI_{DL}$ to refer to the smoothed time-series of NDVI.

2.2.2 Fraction of canopy absorbed PAR and relationships with NDVI

The fraction canopy absorbed PAR ($fAPAR_{canopy}$) was measured at a spectral tower located in birch forest north-west from

5   Abisko village (Fig. 1, black star). $fAPAR_{canopy}$ was obtained using the four-component method, i.e. measurements of incoming PAR above canopy, the total reflected PAR above the canopy, the transmitted PAR below the canopy, and the reflected PAR by the understorey vegetation and ground below the canopy. See Eklundh et al. (2011) for detailed information about the estimation of the pure canopy absorbed PAR. All PAR sensors were calibrated at the field site following the procedure by Jin & Eklundh (2015), and $fAPAR_{canopy}$ at solar noon time was calculated and used in the final

10   analysis. $fAPAR_{canopy}$ data were available for the years 2010 and 2011.

An ordinary least squares (OLS) regression was performed to find the relationship between $fAPAR_{canopy}$ and $NDVI_{DL}$, and the linear equation derived was used in the LUE model to obtain fAPAR from the double logistic fitted NDVI.

2.2.3 Eddy covariance and meteorological data

The EC-tower is situated in the eastern part of the study area (Fig. 1, black triangle), and located near the crossing point of

15   four nominal MODIS pixels with 250×250 m spatial resolution (Fig. 2). Vegetation in the four pixels is similar with some open mire in the north east pixel and a paved road crossing the two southernmost pixels. The towers' footprint is estimated to about 200 m which is slightly smaller than a MODIS pixel. The prevailing wind directions are from the west and from the east, hence the main footprint of the EC-tower is to the east and west from the tower where vegetation is most homogenous. Time-series of NDVI were extracted and mean values and standard deviations were computed for the four MODIS pixels to

20   study if there were any larger deviations in the pixels' NDVI signals. In Figure 3, mean NDVI and standard deviation for the four pixels in the period 2010–2014 are shown. The low standard deviations indicate that there are minor differences in the NDVI signal between the pixels during the main growing season for both raw NDVI and $NDVI_{DL}$ both for years without disturbance and for outbreak years. Hence, we assume that a varying footprint of the EC-tower due to varying wind directions and wind speeds will have a limited influence on the EC measurements.
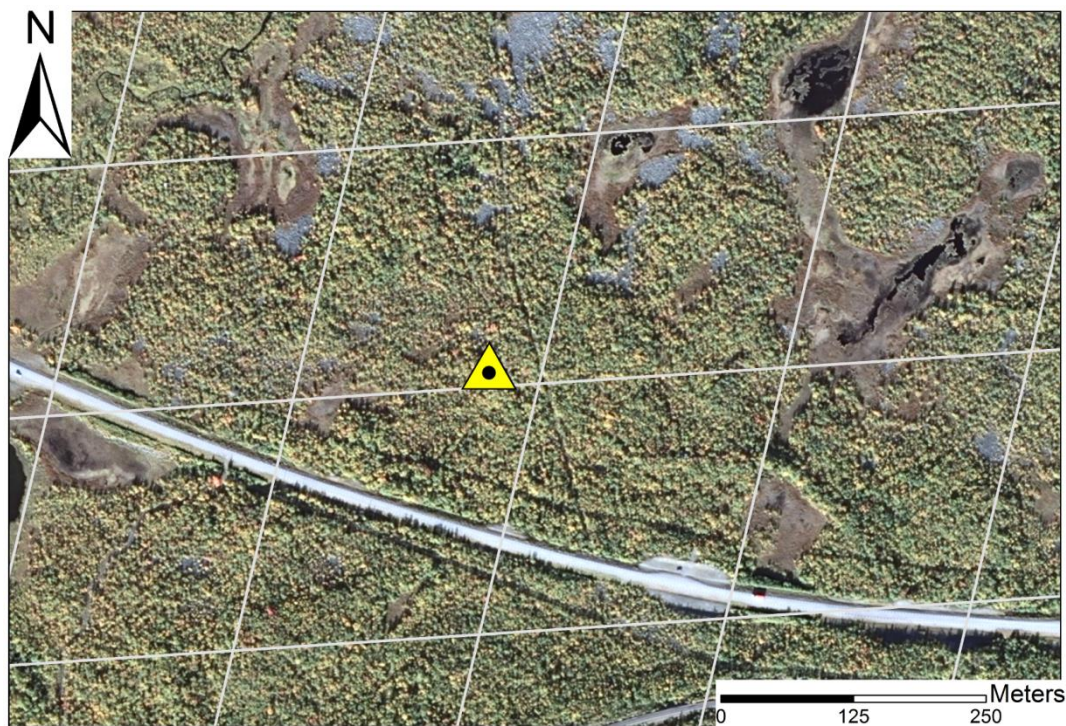
Source: Lantmäteriet Dnr: I2014/00579.

Figure 2. The location of the eddy covariance (EC) tower (yellow triangle) near the crossing point of four nominal MODIS pixels with 250×250 m spatial resolution (white lines). Reference system: SWEREF99 TM. Lantmäteriet (Dnr: I2014/00579).
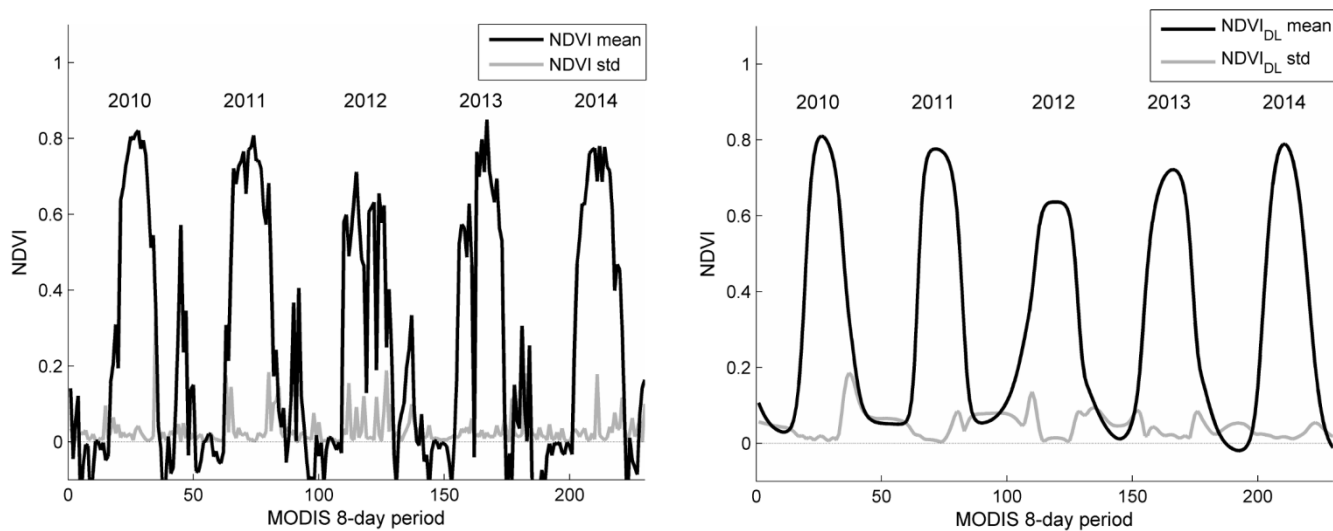
5   **Figure 3. Mean (black) and standard deviation (gray) of NDVI 2010–2014 for the four pixels around the eddy covariance (EC) tower, with raw NDVI to the left, and NDVI fitted with double logistic functions in TIMESAT (NDVI$_{DL}$) to the right. 2012 and 2013 are years with insect outbreak.**

The EC-measurements were made 8 m above ground, 3.3 m above canopy, using a 3-dimensional sonic anemometer (Metek USA-1; METEK Gmbh., Germany) and an open path infrared gas analyzer (Licor 7500, LI-COR Inc., USA). The system was operated with a frequency of 20 Hz and data were recorded by a data logger (CR1000; Campbell Scientific, Inc., USA). Additional measurements of air temperature (Vaisala WXT510; Vaisala, Finland) and incoming photosynthetic flux density

5 (PPFD; JYP 1000, SDEC, France), used for flux partitioning and gap filling, were made at the flux tower. Data were obtained each year during the period May 1 to September 30, which is from before the start of the growing season until late growing season. For the years 2004 and 2013, temperature and PAR were obtained from Abisko scientific research station (ANS); comparisons between data from ANS and the EC-tower showed small differences for the years when data were available from both sources.

10 EC-flux calculations were done with the EddyPro software ver. 5.2.1 (LI-COR Inc., USA). Gaps caused by bad weather conditions, bad EC-measuring conditions, or short breaks in instrument functioning were filled with the online model: Eddy covariance gap-filling & flux-partitioning tool (http://www.bgc-jena.mpg.de/~MDIwork/eddyproc). A model from the same website was used to partition NEE into GPP and ecosystem respiration (R_{eco}). It was assumed that night time NEE is equal to night time R_{eco}. Accordingly, the accepted night-time data were fitted to the Lloyd and Taylor (1994) model based on air

15 temperature. This model was also used to estimate R_{eco} during daytime conditions. GPP was estimated as the residual after subtracting R_{eco} from measured the NEE. Details about gap filling and flux partitioning are described in Reichstein et al. (2005).

2.2.4 Land cover and elevation data

Land cover data were obtained from the Swedish mapping, cadastral, and land registration authority (Lantmäteriet; Dnr:

20 I2014/00579). These land cover data are based on a classification of Landsat TM data and updated in the year 2000 as a part of the CORINE land cover project, but with a finer spatial resolution of 25×25 m (Lantmäteriet 2010). Birch forests in the study area were identified by extracting all pixels with broadleaved forest. Since birch is the dominating tree species with only a few sporadic individuals of other species (Sonesson & Lundberg 1974), all forests were considered to be birch. These data were used to calculate the fraction forest cover per MODIS pixel.

25 Elevation data were obtained from Lantmäteriet as a digital elevation model (DEM) with 50×50 m spatial resolution (Lantmäteriet; Dnr: I2014/00579). Mean elevation for each MODIS pixel was computed as the average altitude of all DEM pixels covered by a MODIS pixel. These data were used to compute altitudinal differences in temperatures when applying the LUE model.

2.3 Light use efficiency model

30 A LUE model with mean values of daily GPP in eight day intervals (GPP_{lue}) (g C m^{-2} day^{-1}), corresponding to the time interval of the MODIS data, was developed as:

$$GPP_{lue} = \varepsilon \times fAPAR_{8day} \times PAR_{8day} \qquad (2)$$

where ε (g C MJ^{-1}) is the light use efficiency, $fAPAR_{8day}$ is fAPAR for a MODIS eight day period derived from $NDVI_{DL}$, and PAR_{8day} (MJ day^{-1}) is mean daily PAR measured at the EC-tower over the eight day period. The light use efficiency was computed as:

$$\varepsilon = \varepsilon_{max} \times f_{8day} \tag{3}$$

5 where ε_{max} is the maximum efficiency applied in the model and f_{8day} is a reduction factor introduced to model the variability in ε depending on temperature. Two models were created to describe f_{8day}, as in Lagergren et al. (2005): One model for the first part of the growing season and one model for the second part of the growing season.

2.3.1 First part of the growing season

During the first part of the growing season, covering May to late June, f_{8day} depended on growing degree days (GDD) and
10 frost events, where GDD was computed with a base temperature of 5°C, following Senn's et al. (1992) method applied to mountain birch development in northern Finland:

$$GDD_t = \begin{cases} GDD_{t-1} & , T_{mean8} \leq 5 \\ GDD_{t-1} + T_{mean8} - 5 & , T_{mean8} > 5 \end{cases} \tag{4}$$

where T_{mean8} (°C) is the mean temperature for a MODIS eight day period. The reduction factor was computed as:

$$f_{8day} = \begin{cases} 1 & , GDD_t \geq GDD_{thres} \\ 1 - \dfrac{GDD_{thres} - S_{GDD}}{GDD_{thres} + S_{GDD}} & , GDD_t < GDD_{thres} \end{cases} \tag{5}$$

15

where GDD_{thres} is a threshold applied to decide when temperature and frost events no longer influence ε, in a similar fashion as Bergh et al. (1998) and Lagergren et al. (2005). S_{GGD} is a reduction factor influenced by GDD and frost events and computed as:

$$S_{GDD} = \frac{GDD_t}{1 + P_{frost}} \tag{6}$$

20 where P_{frost} is a reduction factor controlled by frost events and computed as:

$$P_{frost} = \begin{cases} 0 & , T_{min8} \geq -3 \\ \dfrac{0.05 \times (-3 - T_{min8})}{5} & , T_{min8} < -3 \geq -8 \\ 0.05 & , T_{min8} < -8 \end{cases} \tag{7}$$

where T_{min8} (°C) is the lowest temperature during a MODIS eight day period.

2.3.2 Second part of the growing season

25 In the second part of the growing season, covering late June to September, f_{8day} is controlled by mean temperature only as:

$$f_{8day} = \begin{cases} 1 & , T_{mean8} \geq T_{thres} \\ \dfrac{T_{mean8}}{T_{thres}} & , T_{mean8} < T_{thres} \end{cases} \tag{8}$$

where T_{thres} (°C) is a temperature factor for controlling the influence of the eight day mean temperature during the second part of the growing season.

2.3.3 LUE model optimization

The LUE model was optimized to find three factors: (1) the GDD threshold (GDD_{thres}), (2) the temperature factor (T_{thres}), and (3) the period to change from the first to the second seasonal model, by minimizing the root mean square error (RMS) and maximizing R^2, based on GPP_{lue} and daily mean values of GPP from the EC-tower over MODIS eight day periods (GPP_{EC}). To compute ε_{max}, the mean value of the light use efficiency for all MODIS periods with maximum efficiency i.e. $f_{8day} = 1$ was calculated, where the efficiency was computed as:

$$\varepsilon = \frac{GPP_{EC}}{fAPAR_{8day} \times PAR_{8day}} \tag{9}$$

where GPP_{EC} was derived from the EC-tower. Two ε_{max} values were computed: one including data from the five years with undisturbed birch forest, and one ($\varepsilon_{max, def}$) for the year 2012 with insect defoliation.

2.3.4 LUE model uncertainty

A Monte Carlo approach was applied to evaluate the uncertainty of the LUE model by creating sets with 100 parameter values each for ε_{max} and slope and intercept derived from the OLS regression between $fAPAR_{canopy}$ and $NDVI_{DL}$. The standard deviation of ε_{max} was estimated from all MODIS periods with maximum efficiency, as described in 2.3.3, and a 95% confidence interval for the regression line was estimated. The different sets of parameters were created randomly from a uniform distribution, and the Monte Carlo simulation was run for all possible combinations of parameter values for the five years with undisturbed forests and over 15 sets of 100 MODIS pixels with birch forest. Mean and standard deviation of LUE modelled GPP were estimated from these simulations.

2.4 Identifying MODIS pixels with defoliated birch forest

Defoliated MODIS pixels were identified for the three years with insect outbreaks with a near real-time monitoring method based on Kalman filtering and cumulative sums (Olsson et al. 2016). The method identifies a seasonal trajectory of NDVI representing birch forest during a year without disturbances, called *stable season*. A Kalman filter (Kalman 1960) is applied to the raw NDVI observations from the year of study and deviations from the stable season are computed. A cumulative sum (CUSUM) filter (Page 1954) is applied to these deviations, and a pixel is classified as defoliated when the cumulative sum of deviations reaches a given threshold. In a near real-time application the stable season can only be derived from years prior to

the year of study. In this study we modified the method so that the stable season was derived from all years with available data. For high detection accuracy, the method requires that a MODIS pixel is covered by at least 50% forest. Hence, based on the land cover data from Lantmäteriet, forest in pixels with lower forest cover were excluded, resulting in 100 km^2 of the totally 125 km^2 birch forest in the study area being included; the mean forest cover was 80% per MODIS pixel. The method

5 detected 74% of the defoliated sampling areas in the study area with a misclassification of undisturbed areas of 39% (Olsson et al. 2016).

2.5 Annual GPP loss due to insect defoliation

The LUE model was applied to all MODIS pixels with a forest cover of at least 50%. To adjust for altitudinal differences in temperatures across the study area, a mean summer temperature gradient of 0.5°C per 100 m (Josefsson 1990; Holmgren &

10 Tjus 1996) was applied to the temperature data from the EC-tower. We considered the eight day average of incoming PAR (PAR_{8day}), measured at the EC-tower, to be valid for all pixels in the study area; comparisons between PAR measured at the EC-tower and Abisko scientific research station also showed that average PAR is similar. GPP for a year without insect defoliation was estimated for all pixels by applying the LUE model and computing the mean value for the five years without insect outbreak, and with data available from the EC-tower.

15 Two methods were applied to study the reduction in annual GPP due to the insect outbreaks: (1) a method based on a reduction factor derived from the EC-data and applied to all pixels in the study area, and (2) a method where the LUE model was applied to all defoliated pixels with $\varepsilon_{max, def}$ computed for defoliated growing seasons, and where the loss in GPP was computed as the difference between undisturbed and defoliated years.

2.5.1 Method 1 - GPP reduction factor

20 The fraction of the measured annual GPP at the EC-tower that was lost due to the insect outbreak in 2012 ($GPP_{reduction}$) was computed as:

$$GPP_{reduction} = 1 - GPP_{defoliated}/GPP_{undisturbed} \qquad (10)$$

where $GPP_{defoliated}$ is annual GPP from the EC-tower in 2012. $GPP_{undisturbed}$ is GPP from the tower representing a year without disturbances and computed as the mean of annual GPP for the five years without disturbances.

25 The reduction in annual GPP was computed for each pixel by applying the reduction factor to GPP for undisturbed years and multiplying with the area forest cover in the pixel. The same reduction factor was applied to all years with insect defoliation. The total impact on carbon uptake was computed as the sum of GPP loss for all defoliated pixels in the study area, and for each year with insect outbreak.

2.5.2 Method 2 - LUE model for defoliated pixels

30 The LUE model, modified to model growing season with defoliation, was applied to all defoliated pixels in the study area to estimate annual GPP for each year with defoliation. Derivation of $\varepsilon_{max, def}$ was done with the same method as ε_{max}, but only data from the insect outbreak in 2012 were available to estimate $\varepsilon_{max, def}$, and to evaluate the performance of the defoliation

LUE model. The total reduction in GPP was computed by summing the differences between GPP for healthy years and GPP for defoliated years for all pixels identified as defoliated.

2.5.3 Influence of refoliation

We also studied how recovering foliage later in the growing season influenced the two methods. The assumption was that recovering foliage would result in slightly higher $NDVI_{DL}$ values, which would enable Method 2 to capture the refoliation and hence, estimate GPP losses more accurate. All pixels that were detected as defoliated were classified as refoliated or non-refoliated with the defoliation monitoring method. The differences between GPP loss derived with method 1 and method 2 were computed as *GPP loss method 1 - GPP loss method 2*. Finally, the mean differences for refoliated and non-refoliated pixels were derived.

3 Results

3.1 Correlation between fAPAR and NDVI

There was a strong linear relationship between $fAPAR_{canopy}$ and $NDVI_{DL}$ for $NDVI_{DL}$ values ≥ 0.4 (Fig. 4). The influence of $NDVI_{DL}$ values < 0.4 and with $f_{8day} > 0$ was small, including only 1.1% of the observations and with an average f_{8day} of 0.25. Hence, an OLS regression was performed with $NDVI_{DL}$ values ≥ 0.4 to model the relationship between *fAPAR* and $NDVI_{DL}$. This resulted in an R^2 of 0.81 and the relationship:

$fAPAR = -0.05 + 0.60 \times NDVI_{DL}$

The 95% confidence intervals for slope and intercept applied in the Monte Carlo simulation to estimate the LUE model's uncertainty were -0.05 ±0.18 (intercept) and 0.60 ±0.11 (slope).
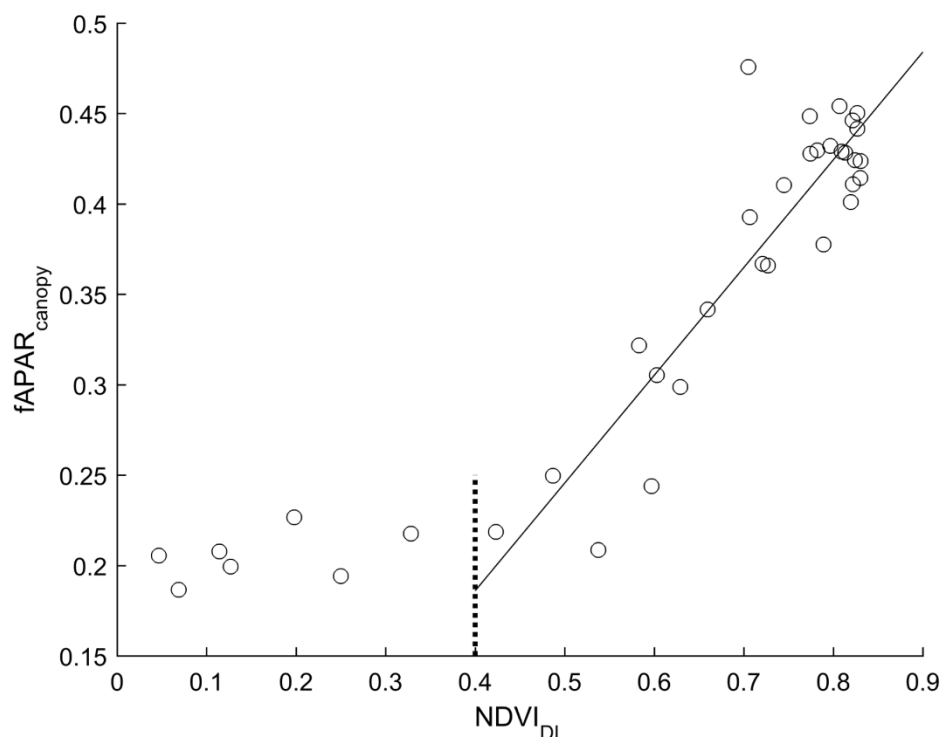
Figure 4. Correlation between ground measured canopy absorbed PAR (fAPAR$_{canopy}$) and MODIS derived NDVI smoothed with a double logistic function in TIMESAT (NDVI$_{DL}$) in eight days intervals. Only NDVI$_{DL}$ values ≥ 0.4 were included in the OLS regression resulting in the black line. R^2 = 0.81 and N = 29.

5   **3.2 Light use efficiency**

Optimization resulted in a GDD threshold of 32 growing degree days (Fig. 5, left) and a temperature factor of 8°C (Fig. 5, middle). The optimal period to change the model for f_{8day} was after MODIS period 23 i.e. the last week of June (Fig. 5, right).
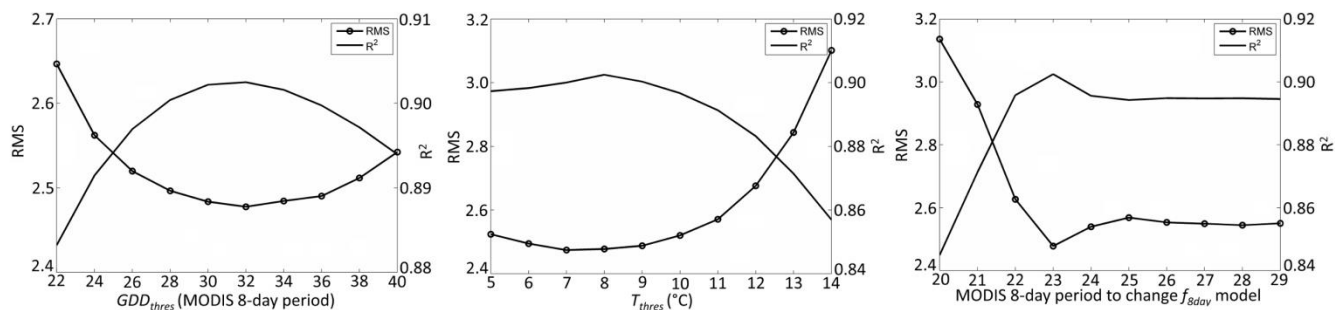

10   **Figure 5. Influence on RMS and R^2 of GDD$_{thres}$ (left), T$_{thres}$ (middle), and the optimal period to change from the first to the second f_{8day} model (right).**

Light use efficiency for years with no disturbance and with $f_{8day} = 1$ (black line with error bars in Fig. 6)) gave an ε_{max} of 1.85 ±0.36 g C MJ^{-1} (±1 standard deviation), resulting in the following LUE model:

$$GPP_{lue} = 1.85 \times f_{8day} \cdot (-0.05 + 0.60 \times NDVI_{DL}) \times PAR_{8day}$$

5   The correlation between GPP_{EC} and GPP_{lue} was strong with $R^2 = 0.90$ (Figure 7). The low GPP observations are mainly from May, before the growing season had started, and have little influence on annual GPP. The Monte Carlo simulation resulted in an estimated standard deviation of 30% of the mean annual GPP. Hence, all annual GPP values derived from the LUE model are given with a standard deviation of 30% of annual GPP.
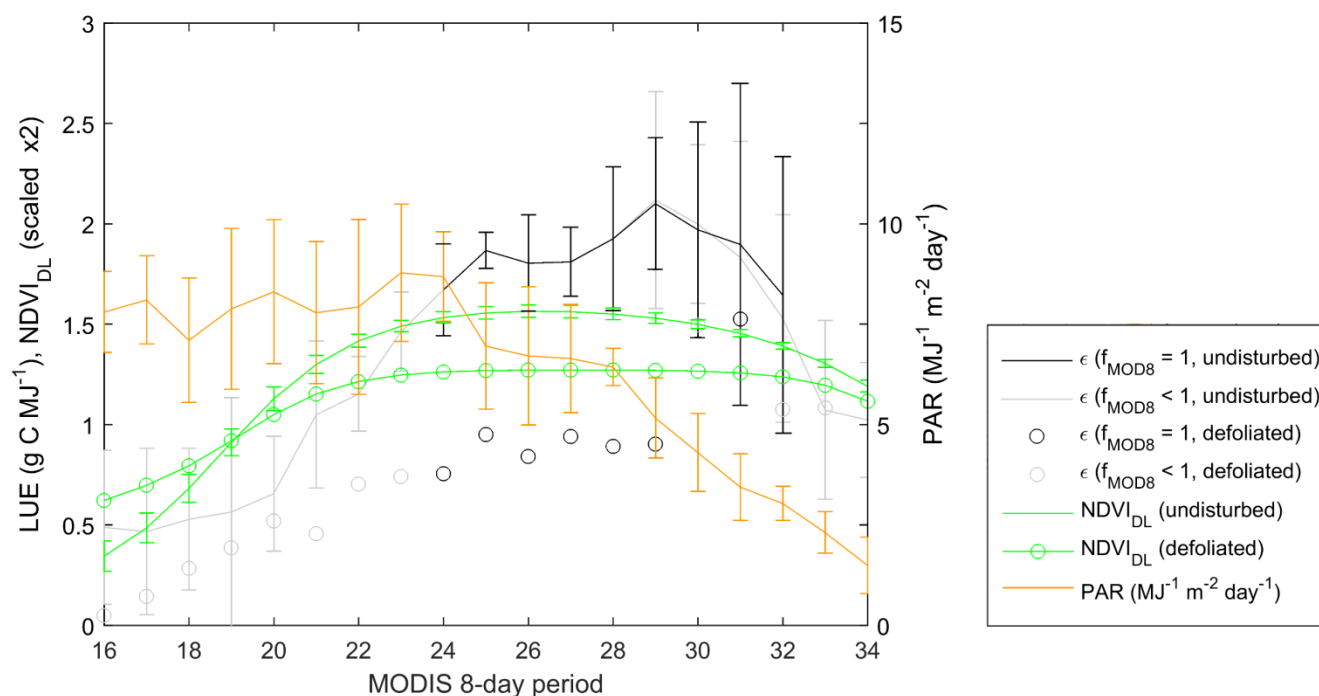
Figure 6. Light use efficiency (ε), NDVI fitted with double logistic functions (NDVI$_{DL}$) scaled ×2 (green), and PAR (orange) for the six years with data from the EC-tower. Black lines with error bars and black circles are the light use efficiency values included when ε$_{max}$ and ε$_{max, def}$ were computed for undisturbed and defoliated years respectively. The error bars are symmetric and one standard deviation higher or lower than the mean values.
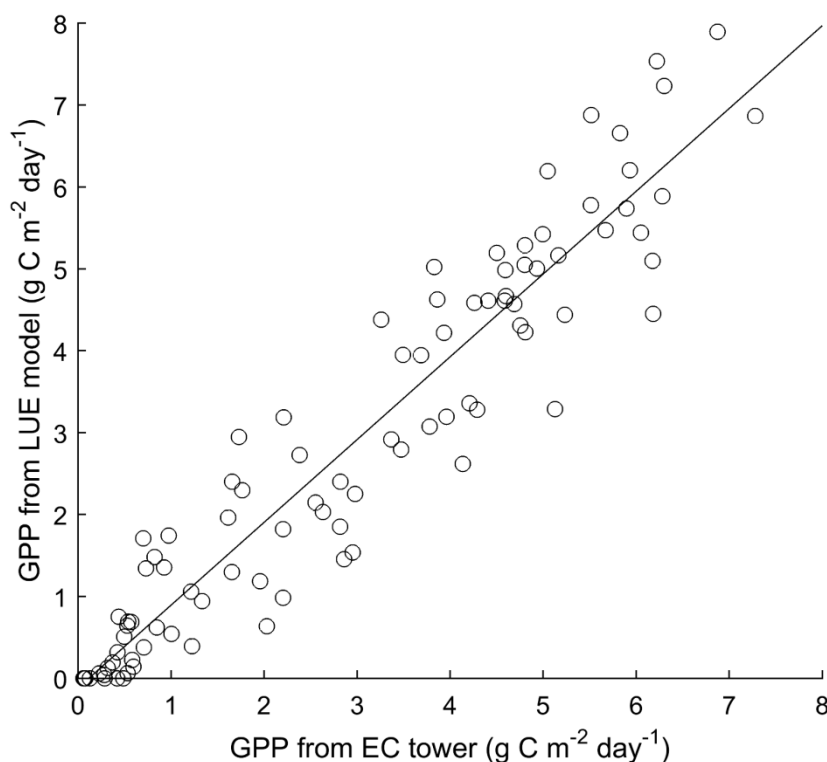
14

Figure 7. Correlation between GPP from the EC-tower and LUE modelled GPP for the five years with undisturbed forests. R^2 = 0.90 and N = 95.

3.3 Impact of insect outbreaks on annual GPP

5 **3.3.1 Reduction factor and LUE model applied to quantify loss in GPP**

Method 1 - reduction factor

GPP measured from the EC-tower and the five years with available data (Table 1) resulted in a mean annual GPP of 441 g C m^{-2}. During the outbreak in 2012 annual GPP was 180 g C m^{-2} which resulted in a reduction in GPP compared to undisturbed conditions of 59%. Hence, a factor *GPP$_{reduction}$* = 0.59 was applied to quantify the impact of the insect outbreak

10 on the carbon balance.

Table 1. Annual GPP derived from the EC-tower for the five years without insect outbreak and the year 2012 with insect outbreak.

|	Years without insect outbreak					Outbreak
Year	2007	2009	2010	2011	2014	2012
GPP (g C m^{-2} yr^{-1})	451	401	448	531	373	180

Biogeosciences
Discussions

Open Access

EGU

Method 2 - LUE model for defoliated pixels

The correlation between GPP_{EC} and GPP_{lue} for the year with defoliation (2012) and data available from the EC-tower was weaker than for years without disturbances (Fig. 8). R^2 was 0.83 and the light use efficiency for the MODIS eight day periods with $f_{8day} = 1$ (black circles in Figure 6) gave an $\varepsilon_{max,\,def}$ of 0.98 ±0.25 g C MJ^{-1} (±1 standard deviation), resulting in the following LUE model for defoliated pixels:

$GPP_{lue,\,defoliated} = 0.98 \times f_{8day} \cdot (\text{-}0.05 + 0.60 \times NDVI_{DL}) \times PAR_{8day}$

The Monte Carlo simulation resulted in an estimated standard deviation of 35% of the mean annual GPP for years with defoliation. Hence, all annual GPP losses estimated with model 2 are given with a standard deviation of 35%.
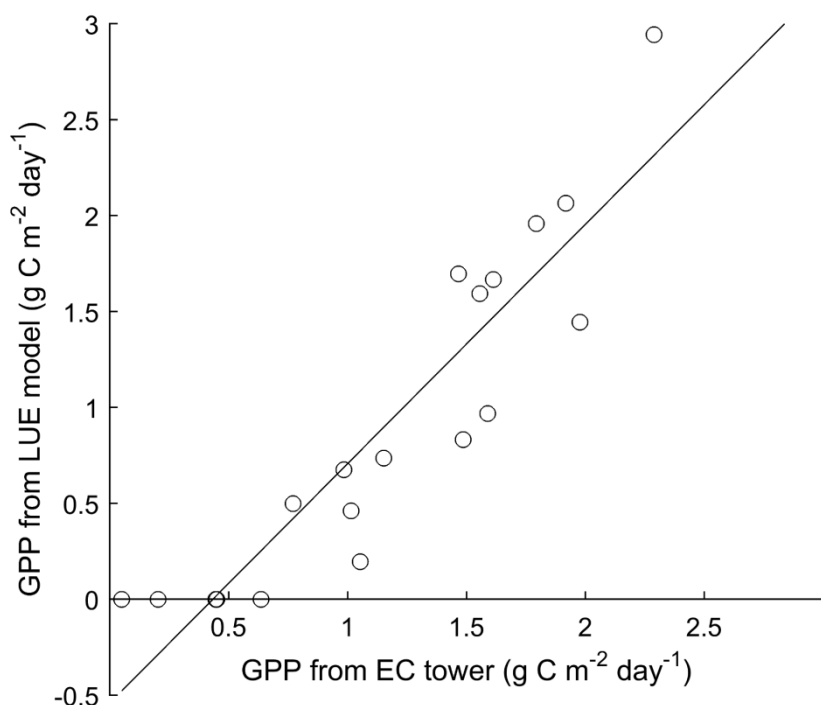
Figure 8. Correlation between GPP from the EC-tower and LUE modelled GPP for the year 2012, with insect outbreak. R^2 = 0.83 and N = 19.

3.3.2 Defoliated areas and quantifying the insect outbreaks impact on annual GPP

In the year 2012, with the most widespread defoliation in this study, 76% of the 100 km^2 forests were defoliated (Table 2 and Fig. 9). In 2004 and 2013, 53% and 55% respectively, of the forests were defoliated. The defoliation detection method enables detection of 74% of the defoliation with a misclassification of undisturbed areas of 39% (Olsson et al. 2016). The total reduction in carbon uptake due to the insect outbreaks since the year 2000 was 44.6 ±13 Gg C according to Method 1,
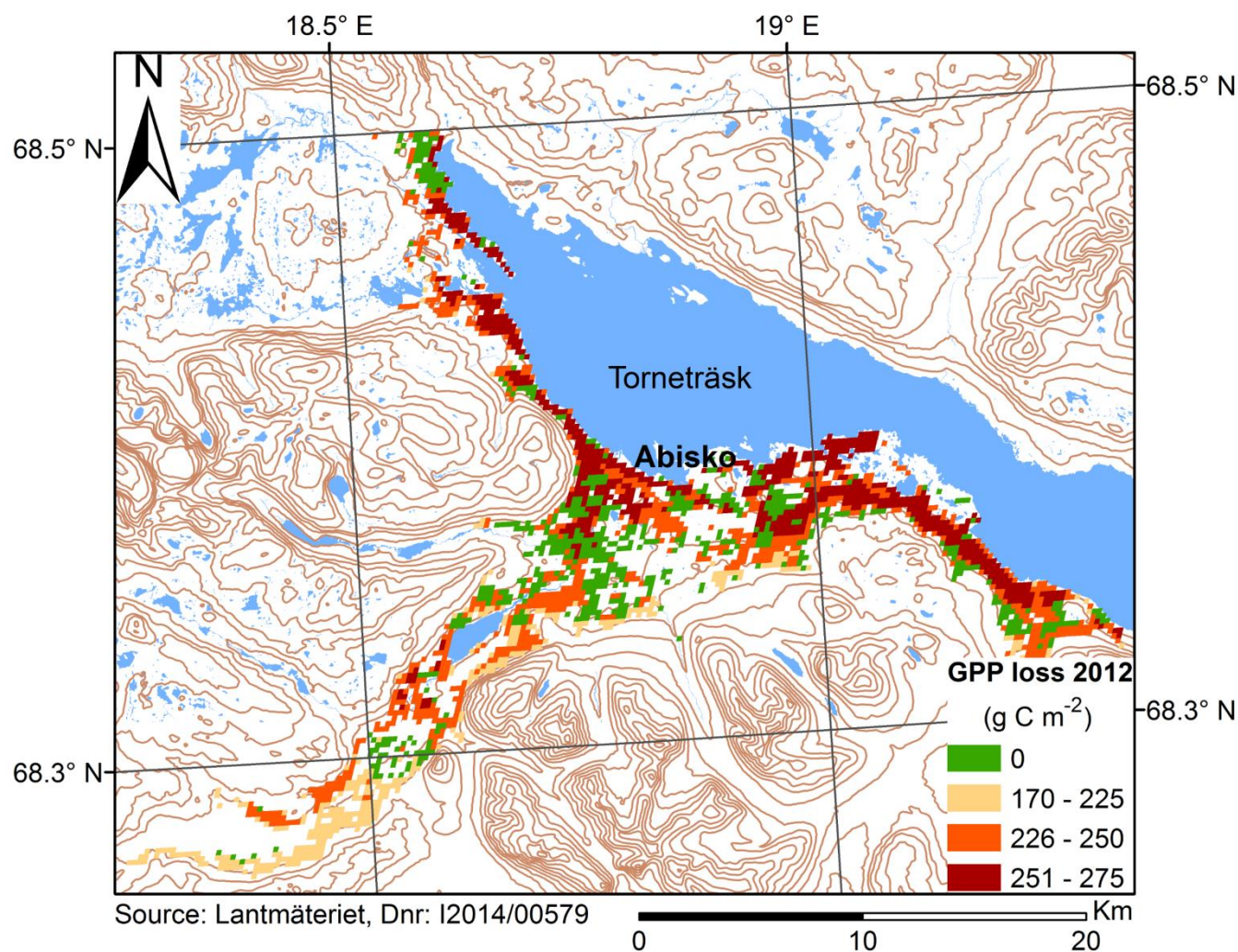
with the largest outbreak in 2012 with a negative impact on GPP of 18.4 ±6 Gg C (Table 2). The average annual GPP in the study area, according the LUE model, was 41.1 ±12 Gg C, which gives a reduction in 2012 of 45%. The impacts of the outbreaks in 2004 and 2013 were reduction in GPP of 31% and 33% respectively. There were only minor differences in the GPP reduction per square meter, ranging from 240 ±72 g C m^{-2} in 2004 to 244 ±73 g C m^{-2} in 2013. Since a common

5   reduction factor is used the results show that in 2013 MODIS pixels with slightly higher GPP during undisturbed conditions were defoliated.

When a LUE model was applied to model GPP also during defoliation events (Method 2) the total decrease in GPP was 43.7 ±15 Gg C which is nearly the same estimate as with Method 1. The GPP loss in 2012 was 20.1 ±7 Gg C which is slightly higher compared to Method 1. Year 2004 followed the same pattern with a slightly larger decrease in GPP for

10   Method 2, while the year 2013 resulted in larger decrease in GPP with Method 1. Differences in GPP loss per square meter between the years were larger with Method 2: 188 ±66 g C m^{-2} in 2013 was the lowest GPP loss, and 265 ±93 g C m^{-2} in 2012 was the largest GPP loss.

Table 2. Defoliated area (km^2) and annual reduction in GPP (Gg C) for the three years with insect defoliation since the year 2000. The total area with forest cover was 100 km^2.

Year		2004	2012	2013
	Defoliated area (km^2)	53	76	55
GPP decrease	Mean (g C m^{-2} yr^{-1})	240 ±72	242 ±72	244 ±73
Method 1	Total (Gg C yr^{-1})	12.7 ±4	18.4 ±5	13.5 ±4
(GPP reduction factor)	Total (%)	31	45	33
GPP decrease	Mean (g C m^{-2} yr^{-1})	252 ±88	265 ±93	188 ±66
Method 2	Total (Gg C yr^{-1})	13.3 ±5	20.1 ±7	10.3 ±4
(Defoliation LUE model)	Total (%)	33	49.0	25

Figure 9. Reduction in annual GPP (g C m^{-2}) due to the birch moth outbreak in 2012 computed with a LUE model also for defoliation (Method 2). One standard deviation of the GPP losses is estimated to 35% of the given values. Areas with only the background map have a canopy cover less than 50% or are outside the study area shown in Fig. 1. The reference system is
5 **SWEREF99 TM and latitude and longitude are in WGS84. Source of background map: Lantmäteriet (Dnr: I2014/00579).**

We compared the differences in GPP decrease between Method 1 (GPP reduction factor) and Method 2 (two LUE models) to study if Method 2 performed better for MODIS pixels where the birch trees recovered later in the growing season. For the years 2004 and 2012 the mean differences in GPP loss (g C m^{-2}) between the methods were lower for pixels that recovered later in the growing season. These results suggest that Method 2 captured some of the refoliation, though the differences are

10 small. For 2013, on the other hand, Method 1 resulted in higher value for refoliated pixels, but the difference was minor.

Table 3. Differences in GPP loss (g C m^{-2} yr^{-1}) between Method 1 and Method 2 for MODIS pixels with recovering foliage later in the season, and pixels with no refoliation according to the defoliation monitoring method. Higher GPP loss with Method 2 gives negative values.

18

Year	2004	2012	2013
Refoliated pixels	48%	14%	52%
Difference, refoliated (g C m^{-2} yr^{-1})	-9 ±3	-19 ±7	57 ±20
Difference, non-refoliated (g C m^{-2} yr^{-1})	-15 ±5	-24 ±8	54 ±19

4 Discussion

This study has demonstrated a substantial setback to the carbon uptake caused by insect defoliation in a subarctic deciduous forest in northern Fennoscandia. At the EC-tower, GPP decreased with 260 g C m^{-2} (59%) during the outbreak in 2012 compared to the mean of undisturbed years. In the entire study area annual mean values of decrease in GPP ranged from

5 188 ±66 to 244 ±73 g C m^{-2}. The total decrease in carbon uptake, due to the insect defoliation events since the year 2000 was estimated to be 44.6 ±13 Gg C, which is of the same magnitude as the average annual GPP of 41.1 ±12 Gg C for single years with no disturbances. These figures are likely conservative; 20% of the forests in the study area were excluded since they are located in MODIS pixels with < 50% forests cover. During the most severe outbreak year (2012), the annual GPP loss was nearly 50% (20 Gg C), with 76% of the 100 km^2 birch forests in the study area defoliated. This study also highlights the

10 advantage of combining EC-data and remote sensing data where data from the EC-tower were applied to calibrate the LUE model, and satellite data were applied to estimate the impact on GPP over larger areas. EC-measurement alone cannot be extrapolated with high accuracy if the spatial and temporal extent of an outbreak is unknown, and the LUE model could not be developed without available EC-data. The combination facilitates wall-to-wall mapping of disturbances in forests, and quantitative estimates of the impacts on primary productivity.

15 The two methods applied to quantify the impacts on GPP resulted in similar total GPP losses for the outbreaks, but with annual differences in GPP losses for the outbreak years. The assumption was that Method 2 would be more adaptive and adjust for differences in defoliation intensities between MODIS pixels. Since the level of defoliation, as well as understorey responses to the defoliation are likely to influence $NDVI_{DL}$, which in turn will influence $fAPAR$, it was anticipated that a method based on a LUE model to derive GPP during defoliation events would capture variability in defoliation levels and

20 understory responses between MODIS pixels. Method 1, on the other hand, with a common reduction factor, does not account for local differences between pixels and is similar to upscaling the local conditions at the EC-tower, even though the method has the advantage that annual GPP for each pixel is derived with a LUE model and hence, should be more accurate than assuming that GPP for all MODIS pixels is identical to GPP at the EC-tower. For the year 2012, when there was little refoliation in the area (Table 3), Methods 1 and 2 resulted in similar estimates of the GPP loss with slightly larger decrease in GPP for Method 2. Both methods resulted in similar GPP reductions, with marginally larger decrease for Method 2, also

25 in GPP for Method 2. Both methods resulted in similar GPP reductions, with marginally larger decrease for Method 2, also for the year 2004 when refoliation was widespread in the study area (Table 3). The larger difference between the methods in 2013 could be due to substantial refoliation, which was captured by method 2, and which resulted in a lower GPP reduction. However, since there was refoliation also in the year 2004, when there were only minor differences between Method 1 and 2,

the large differences could also be due to uncertainties in $\varepsilon_{max,\,def}$, which was estimated from one year with defoliation only. It should also be noted that higher NDVI might be due to increasing growth of understory grasses favoured by the changed light conditions due to defoliation (Karlsen et al. 2013) rather than recovering birch. More data from the EC-tower would be required to confirm this. It is, however, likely that Method 2 will result in more accurate estimates of the decrease in GPP if

5   data are available to make more robust estimates of $\varepsilon_{max,\,def}$.

A limitation with the developed LUE model for large-area estimates is that it includes observed meteorological data (temperature and PAR). An alternative for running the model over larger areas would be to use modelled meteorological data (Olofsson et al. 2007; Schubert et al. 2010). There are also uncertainties related to the temperature data utilized. The gradient applied to model mean temperatures depending on altitude is likely to give accurate estimates in the study area. However,

10 minimum temperatures are more uncertain since cold air can drain downhill and accumulate in valleys and low areas, rather than decrease with altitude. Altogether, since the EC-tower is located on a small ridge in the lower, flat parts of the study area, we anticipate that the temperatures there are not substantially lower than the area in general. We compared with lowest daily temperature from Abisko research station, which is located near the spectral tower 10 km to the west (Fig. 1), and at a slightly higher altitude than the EC-tower. For all periods with frost events during the early season, i.e. when the lowest

15 temperature influences f_{MOD8}, the mean value of absolute differences, with the coldest temperatures at the research station, was only 0.4°C. With these small temperature differences and since frost events only influence GPP in the early growing season, the impact on annual GPP was considered minor.

The impact of insect outbreaks on the carbon balance has been quantified in earlier studies: Heliasz et al. (2011) studied the impact on NEE of the autumnal moth and winter moth outbreak in Abisko in 2004, but these measurements started on July 2,

20 which was around 10 days after the larvae reached peak densities, which most likely resulted in an underestimated reduction in NEE. To facilitate a comparison between the outbreak years 2004 and 2012, we computed GPP for the period July 2 to September 30 for all years with EC-data. This indicated that the two outbreak years had similar impact on the carbon balance during the period studied with a GPP loss of 205 g C m^{-2} in 2004 and 199 g C m^{-2} in 2012 compared to years without disturbance. Furthermore, the loss of 199 g C m^{-2} in the year 2012 and for the same time period as studied in the year 2004,

25 compared to the GPP loss of 260 g C m^{-2} for the entire growing season in 2012, suggests that the impact on NEE was underestimated by Heliasz et al. (2011). Clark et al. (2010) found the highest difference in NEE between undisturbed years and years with severe defoliation by the gypsy moth in New Jersey, USA, to be 266–480 g C m^{-2} and Clark et al (2014) found that mid-day NEE during complete defoliation was 14% of pre-defoliation rates. Allard et al. (2008) noted that cumulative NEE was lower during a year with insect defoliation compared to years without disturbances; however, the low

30 NEE value might to a large extent have been caused by a dry spring. Brown et al. (2010) found that a mountain pine beetle outbreak turned a forest into a carbon sink; no pre-outbreak EC-data were available to quantify the impact on NEP, but recovery after the outbreak was faster than anticipated (Brown et al. 2012). It should be noted that the mountain pine beetle feed within the phloem and directly kills trees, while the moth species discussed above are defoliators that usually only kill trees in cases of severe and repeated outbreaks (Hicke et al. 2012). Modeling studies have also found that forests have

changed from sinks into sources of carbon, in some cases for extended periods (Kurz et al. 2008a; Dymond et al. 2010; Schäfer et al. 2010; Medvigy et al. 2012). However, to our knowledge, this is the first study that has utilized remote sensing data and applied a LUE model, calibrated with EC-data, to both quantify and map the spatial extent of the impact of insect outbreaks on GPP.

5 The results of this study could help to reduce uncertainties in the impact of insect outbreaks on primary productivity as well as to improve carbon budgets by including insect induced defoliation. For the mountain birch forests in this study the estimated reduction in annual GPP, compared to years without disturbances, was 50% when there was limited refoliation in the study area. For years with widespread refoliation, the annual GPP losses were about 1/3 of GPP for years without disturbances. In addition, the spatial and temporal mapping of insect defoliation provided by remote sensing is important for

10 accurate simulation of the carbon dynamics, since it has been suggested that the spatial distribution of defoliation has a strong influence on carbon dynamics (Medigvy et al. 2012). Furthermore, the outbreak area included in this study is only a fraction of the 10,000 km^2 estimated to having been severely defoliated in northern Fennoscandia during the period 2000–2008 (Jepsen et al. 2009). Extrapolating the reduction in annual GPP over these vast defoliated areas would result in a GPP loss of the magnitude 2–3 Tg C in northern Fennoscandia for that time period. Models not accounting for such disturbance

15 events would seriously overestimate the ability of these forests to absorb atmospheric CO_2.

5 Conclusions

This study demonstrated, with the aid of MODIS NDVI and eddy covariance data, a substantial loss in GPP due to insect induced defoliation in subarctic deciduous forest in northern Fennoscandia. The estimated total decrease in GPP in the study area of 100 km^2 due to insect outbreaks since the year 2000 was 44.6 ±13 Gg C for three disturbance events, comparable

20 with the average annual GPP of 41.1 ±12 Gg C for years without disturbances. In the most severe outbreak year (2012) 76% of the birch forests were defoliated and annual GPP was merely 50% of GPP for years without disturbances.

The study also demonstrated the use of remote sensing data to both monitor the spatial extent of the defoliation and to estimate the impact on the primary productivity of these defoliation events. The insect disturbance is shown to have major impacts on the primary production of the sub-arctic forest; consequently, the derived methods, based on combining remote

25 sensing and eddy covariance measurements, are of major importance to support carbon balance estimates over large areas.

The authors declare that they have no conflict of interest.

BIOGEOSCIENCES Open Access
Discussions

EGU

References

5 Abisko Scientific Research Station: Temperature data, 1913-2014, 2015. Available from Abisko Scientific Research Station. http://www.polar.se/abisko.

Adelabu, S., Mutanga, O., and Cho, M. A.: A review of remote sensing of insect defoliation and its implications for the detection and mapping of Imbrasia belina defoliation of Mopane Woodland, Afr. J. Plant Sci. Biotechnol, 6, 1-13, 2012.

Allard, V., Ourcival, J. M., Rambal, S., Joffre, R., and Rocheteau, A.: Seasonal and annual variation of carbon exchange in

10 an evergreen Mediterranean forest in southern France, Global Change Biology, 14, 714-725, 10.1111/j.1365-2486.2008.01539.x, 2008.

Ammunét, T., Bylund, H., & Jepsen, J.U.: Northern Geometrids and Climate Change: From Abiotic Factors to Trophic Interactions. In Björkman., C., & Niemelä, P. (Eds.), Climate Change and Insect Pests (pp. 235–247). Boston: CABI, 2015.

Asrar, G., Fuchs, M., Kanemasu, E. T., and Hatfield, J. L.: Estimating Absorbed Photosynthetic Radiation and Leaf Area

15 Index from Spectral Reflectance in Wheat1, Agronomy Journal, 76, 10.2134/agronj1984.00021962007600020029x, 1984.

Babst, F., Esper, J., and Parlow, E.: Landsat TM/ETM+ and tree-ring based assessment of spatiotemporal patterns of the autumnal moth (Epirrita autumnata) in northernmost Fennoscandia, Remote Sensing of Environment, 114, 637-646, http://dx.doi.org/10.1016/j.rse.2009.11.005, 2010.

Battisti, A.: Forests and climate change - lessons from insects, iForest-Biogeosciences and Forestry, 1, 1-5,

20 10.3832/ifor0210-0010001, 2008.

Bergh, J., McMurtrie, R. E., and Linder, S.: Climatic factors controlling the productivity of Norway spruce: a model-based analysis, Forest ecology and management, 110, 127-139, 1998.

Bonan, G. B.: Forests and Climate Change: Forcings, Feedbacks, and the Climate Benefits of Forests, Science, 320, 1444-1449, 10.1126/science.1155121, 2008.

25 Brown, M., Black, T. A., Nesic, Z., Foord, V. N., Spittlehouse, D. L., Fredeen, A. L., Grant, N. J., Burton, P. J., and Trofymow, J. A.: Impact of mountain pine beetle on the net ecosystem production of lodgepole pine stands in British Columbia, Agricultural and Forest Meteorology, 150, 254-264, http://dx.doi.org/10.1016/j.agrformet.2009.11.008, 2010.

Brown, M. G., Black, T. A., Nesic, Z., Fredeen, A. L., Foord, V. N., Spittlehouse, D. L., Bowler, R., Burton, P. J., Trofymow, J. A., Grant, N. J., and Lessard, D.: The carbon balance of two lodgepole pine stands recovering from mountain

30 pine   beetle   attack   in   British   Columbia,   Agricultural   and   Forest   Meteorology,   153,   82-93, http://dx.doi.org/10.1016/j.agrformet.2011.07.010, 2012.

Bylund, H.: Long-term interactions between the autumnal moth and mountain birch: the role of resources, competitors, natural enemies, and weather. , PhD, Swedish University of Agricultural Sciences, 1995.

Callaghan, T. V., Bergholm, F., Christensen, T. R., Jonasson, C., Kokfelt, U., and Johansson, M.: A new climate era in the sub-Arctic: Accelerating climate changes and multiple impacts, Geophysical Research Letters, 37, L14705, 10.1029/2009GL042064, 2010.

Clark, K. L., Skowronski, N., and Hom, J.: Invasive insects impact forest carbon dynamics, Global Change Biology, 16, 88-101, 10.1111/j.1365-2486.2009.01983.x, 2010.

Clark, K. L., Skowronski, N. S., Gallagher, M. R., Renninger, H., and Schäfer, K. V. R.: Contrasting effects of invasive insects and fire on ecosystem water use efficiency, Biogeosciences, 11, 6509-6523, 10.5194/bg-11-6509-2014, 2014.

Dymond, C. C., Neilson, E. T., Stinson, G., Porter, K., MacLean, D. A., Gray, D. R., Campagna, M., and Kurz, W. A.: Future Spruce Budworm Outbreak May Create a Carbon Source in Eastern Canadian Forests, Ecosystems, 13, 917-931, 10.1007/s10021-010-9364-z, 2010.

Eklundh, L., Jin, H., Schubert, P., Guzinski, R., and Heliasz, M.: An Optical Sensor Network for Vegetation Phenology Monitoring and Satellite Data Calibration, Sensors, 11, 7678, 2011.

Field, C. B., Randerson, J. T., and Malmström, C. M.: Global net primary production: Combining ecology and remote sensing, Remote Sensing of Environment, 51, 74-88, http://dx.doi.org/10.1016/0034-4257(94)00066-V, 1995.

Gamon, J. A.: Reviews and Syntheses: optical sampling of the flux tower footprint, Biogeosciences, 12, 4509-4523, 10.5194/bg-12-4509-2015, 2015.

Goodale, C. L., Apps, M. J., Birdsey, R. A., Field, C. B., Heath, L. S., Houghton, R. A., Jenkins, J. C., Kohlmaier, G. H., Kurz, W., Liu, S., Nabuurs, G.-J., Nilsson, S., and Shvidenko, A. Z.: Forest Carbon Sinks in the Northern Hemisphere, Ecological Applications, 12, 891-899, 10.1890/1051-0761(2002)012[0891:FCSITN]2.0.CO;2, 2002.

Goward, S. N., and Huemmrich, K. F.: Vegetation canopy PAR absorptance and the normalized difference vegetation index: An assessment using the SAIL model, Remote Sensing of Environment, 39, 119-140, http://dx.doi.org/10.1016/0034-4257(92)90131-3, 1992.

Heliasz, M., Johansson, T., Lindroth, A., Mölder, M., Mastepanov, M., Friborg, T., Callaghan, T. V., and Christensen, T. R.: Quantification of C uptake in subarctic birch forest after setback by an extreme insect outbreak, Geophysical Research Letters, 38, L01704, 10.1029/2010gl044733, 2011.

Hicke, J. A., Allen, C. D., Desai, A. R., Dietze, M. C., Hall, R. J., Hogg, E. H., Kashian, D. M., Moore, D., Raffa, K. F., Sturrock, R. N., and Vogelmann, J.: Effects of biotic disturbances on forest carbon cycling in the United States and Canada, Global Change Biology, 18, 7-34, 10.1111/j.1365-2486.2011.02543.x, 2012.

Holmgren, B., and Tjus, M.: Summer Air Temperatures and Tree Line Dynamics at Abisko, Ecological Bulletins, 159-169, 1996.

Interact: Abisko Scientific Research Station, 2016. http://www.eu-interact.org/field-sites/sweden-2/abisko/ (accessed 09-02-16).

Biogeosciences Open Access
Discussions
EGU

Jepsen, J. U., Hagen, S. B., Ims, R. A., and Yoccoz, N. G.: Climate change and outbreaks of the geometrids Operophtera brumata and Epirrita autumnata in subarctic birch forest: evidence of a recent outbreak range expansion, The Journal of animal ecology, 77, 257-264, 10.1111/j.1365-2656.2007.01339.x, 2008.

Jepsen, J. U., Hagen, S. B., Høgda, K. A., Ims, R. A., Karlsen, S. R., Tømmervik, H., and Yoccoz, N. G.: Monitoring the spatio-temporal dynamics of geometrid moth outbreaks in birch forest using MODIS-NDVI data, Remote Sensing of Environment, 113, 1939-1947, 2009.

Jepsen, J. U., Biuw, M., Ims, R. A., Kapari, L., Schott, T., Vindstad, O. P. L., and Hagen, S. B.: Ecosystem impacts of a range expanding forest defoliator at the forest-tundra ecotone, Ecosystems, 16, 561-575, 2013.

Jin, H., and Eklundh, L.: In Situ Calibration of Light Sensors for Long-Term Monitoring of Vegetation, IEEE Transactions on Geoscience and Remote Sensing, 53, 3405-3416, 10.1109/TGRS.2014.2375381, 2015.

Josefsson, M.: The Geoecology of Subalpine Heaths in the Abisko Valley, Northern Sweden – A study of periglacial conditions. Uppsala University Report 78, 1990.

Jönsson, P., Eklundh, L.: Seasonality extraction by function fitting to time-series of satellite sensor data, PISCATAWAY, 2002, 1824-1832,

Jönsson, P., Eklundh, L.: TIMESAT—a program for analyzing time-series of satellite sensor data, Computers and Geosciences, 30, 833-845, 10.1016/j.cageo.2004.05.006, 2004.

Kalman, R. E.: A New Approach to Linear Filtering and Prediction Problems, Journal of Fluids Engineering, 82, 35-45, 10.1115/1.3662552, 1960.

Karlsen, S., Jepsen, J., Odland, A., Ims, R., and Elvebakk, A.: Outbreaks by canopy-feeding geometrid moth cause state-dependent shifts in understorey plant communities, Oecologia, 173, 859-870, 10.1007/s00442-013-2648-1, 2013.

Kaukonen, M., Ruotsalainen, A. L., Wäli, P. R., Männistö, M. K., Setälä, H., Saravesi, K., Huusko, K., and Markkola, A.: Moth herbivory enhances resource turnover in subarctic mountain birch forests?, Ecology, 94, 267-272, 2013.

Kurz, W. A., Dymond, C. C., Stinson, G., Rampley, G. J., Neilson, E. T., Carroll, A. L., Ebata, T., and Safranyik, L.: Mountain pine beetle and forest carbon feedback to climate change, Nature, 452, 987-990, http://www.nature.com/nature/journal/v452/n7190/suppinfo/nature06777_S1.html, 2008a.

Kurz, W. A., Stinson, G., and Rampley, G.: Could increased boreal forest ecosystem productivity offset carbon losses from increased disturbances?, Philosophical Transactions of the Royal Society of London B: Biological Sciences, 363, 2259-2268, 10.1098/rstb.2007.2198, 2008b.

Lagergren, F., Eklundh, L., Grelle, A., Lundblad, M., Mölder, M., Lankreijer, H., and Lindroth, A.: Net primary production and light use efficiency in a mixed coniferous forest in Sweden, Plant, Cell & Environment, 28, 412-423, 10.1111/j.1365-3040.2004.01280.x, 2005.

Landry, J. S., Price, D. T., Ramankutty, N., Parrott, L., and Matthews, H. D.: Implementation of a Marauding Insect Module (MIM, version 1.0) in the Integrated BIosphere Simulator (IBIS, version 2.6b4) dynamic vegetation–land surface model, Geosci. Model Dev., 9, 1243-1261, 10.5194/gmd-9-1243-2016, 2016.

Lantmäteriet: Produktbeskrivning: GSD-Marktäckedata, GSD, Geografiska Sverigedata. Dokumentversion 1.2, 2010-03-26, 2010.

Liljedahl, A. K., Hinzman, L. D., Harazono, Y., Zona, D., Tweedie, C. E., Hollister, R. D., Engstrom, R., and Oechel, W. C.: Nonlinear controls on evapotranspiration in arctic coastal wetlands, Biogeosciences, 8, 3375-3389, 10.5194/bg-8-3375-2011, 2011.

Lloyd, J., and Taylor, J. A.: On the Temperature Dependence of Soil Respiration, Functional Ecology, 8, 315-323, 10.2307/2389824, 1994.

LPDAAC: Surface Reflectance 8-Day L3 Global 250m, Land Processes Distributed Active Archive Center, 2016a. https://lpdaac.usgs.gov/dataset_discovery/modis/modis_products_table/mod09q1 (accessed 09-02-16).

LPDAAC: Surface Reflectance 8-Day L3 Global 500m, Land Processes Distributed Active Archive Center, 2016b. https://lpdaac.usgs.gov/dataset_discovery/modis/modis_products_table/mod09a1 (accessed 09-02-16).

McCallum, I., Franklin, O., Moltchanova, E., Merbold, L., Schmullius, C., Shvidenko, A., Schepaschenko, D., and Fritz, S.: Improved light and temperature responses for light-use-efficiency-based GPP models, Biogeosciences, 10, 6577-6590, 10.5194/bg-10-6577-2013, 2013.

Medvigy, D., Clark, K. L., Skowronski, N. S., and Schäfer, K. V. R.: Simulated impacts of insect defoliation on forest carbon dynamics, Environmental Research Letters, 7, 045703, 2012.

Monteith, J. L.: Solar Radiation and Productivity in Tropical Ecosystems, Journal of Applied Ecology, 9, 747-766, 10.2307/2401901, 1972.

Monteith, J. L., and Moss, C. J.: Climate and the Efficiency of Crop Production in Britain [and Discussion], Philosophical Transactions of the Royal Society of London B: Biological Sciences, 281, 277-294, 10.1098/rstb.1977.0140, 1977.

Myneni, R. B., and Williams, D. L.: On the relationship between FAPAR and NDVI, Remote Sensing of Environment, 49, 200-211, 1994.

Nabuurs, G.-J., Lindner, M., Verkerk, P. J., Gunia, K., Deda, P., Michalak, R., and Grassi, G.: First signs of carbon sink saturation in European forest biomass, Nature Clim. Change, 3, 792-796, 10.1038/nclimate1853, 2013.

Netherer, S., and Schopf, A.: Potential effects of climate change on insect herbivores in European forests—General aspects and the pine processionary moth as specific example, Forest Ecology and Management, 259, 831-838, 10.1016/j.foreco.2009.07.034, 2010.

Olofsson, P., and Eklundh, L.: Estimation of absorbed PAR across Scandinavia from satellite measurements. Part II: Modeling and evaluating the fractional absorption, Remote Sensing of Environment, 110, 240-251, 2007.

Olofsson, P., Eklundh, L., Lagergren, F., Jönsson, P., and Lindroth, A.: Estimating net primary production for Scandinavian forests using data from Terra/MODIS, Advances in Space Research, 39, 125-130, http://dx.doi.org/10.1016/j.asr.2006.02.031, 2007.

Olsson, P.-O., Lindström, J., and Eklundh, L.: Near real-time monitoring of insect induced defoliation in subalpine birch forests with MODIS derived NDVI, Remote Sensing of Environment, 181, 42-53, http://dx.doi.org/10.1016/j.rse.2016.03.040, 2016.

Page, E. S.: Continuous Inspection Schemes, Biometrika, 41, 100-115, 10.2307/2333009, 1954.

5 Potter, S. C., Klooster, S., and Brooks, V.: Interannual Variability in Terrestrial Net Primary Production: Exploration of Trends and Controls on Regional to Global Scales, Ecosystems, 2, 36-48, 10.1007/s100219900056, 1999.

Prince, S. D.: A model of regional primary production for use with coarse resolution satellite data, International Journal of Remote Sensing, 12, 1313-1330, 10.1080/01431169108929728, 1991.

Prince, S.D., and Goward, S.N.: Global Primary Production: A Remote Sensing Approach. Journal of Biogeography, 22,

10 815–835, 1995.

Reichstein, M., Falge, E., Baldocchi, D., Papale, D., Aubinet, M., Berbigier, P., Bernhofer, C., Buchmann, N., Gilmanov, T., Granier, A., Grünwald, T., Havránková, K., Ilvesniemi, H., Janous, D., Knohl, A., Laurila, T., Lohila, A., Loustau, D., Matteucci, G., Meyers, T., Miglietta, F., Ourcival, J.-M., Pumpanen, J., Rambal, S., Rotenberg, E., Sanz, M., Tenhunen, J., Seufert, G., Vaccari, F., Vesala, T., Yakir, D., and Valentini, R.: On the separation of net ecosystem exchange into

15 assimilation and ecosystem respiration: review and improved algorithm, Global Change Biology, 11, 1424-1439, 10.1111/j.1365-2486.2005.001002.x, 2005.

Rouse, J. W., Haas, R. H., Shell, J. A., and Deering, D. W.: Monitoring vegetation systems in the Great Plains with ERTS-1, Third Earth Resources Technology Satellite Symposium, 309–317, 1973.

Ruimy, A., Saugier, B., and Dedieu, G.: Methodology for the estimation of terrestrial net primary production from remotely

20 sensed data, Journal of Geophysical Research: Atmospheres, 99, 5263-5283, 1994.

Rullan-Silva, C. D., Olthoff, A. E., Delgado de la Mata, J. A., and Pajares-Alonso, J. A.: Remote Monitoring of Forest Insect Defoliation -A Review, 2013, 22, 15, 10.5424/fs/2013223-04417, 2013.

Running, S. W., Nemani, R. R., Heinsch, F. A., Zhao, M., Reeves, M., and Hashimoto, H.: A Continuous Satellite-Derived Measure of Global Terrestrial Primary Production, BioScience, 54, 547-560, 10.1641/0006-

25 3568(2004)054[0547:ACSMOG]2.0.CO;2, 2004.

Saravesi, K., Aikio, S., Wäli, P. R., Ruotsalainen, A. L., Kaukonen, M., Huusko, K., Suokas, M., Brown, S. P., Jumpponen, A., and Tuomi, J.: Moth Outbreaks Alter Root-Associated Fungal Communities in Subarctic Mountain Birch Forests, Microbial ecology, 69, 788-797, 2015.

Schäfer, K. V. R., Clark, K. L., Skowronski, N., and Hamerlynck, E. P.: Impact of insect defoliation on forest carbon balance

30 as assessed with a canopy assimilation model, Global Change Biology, 16, 546-560, 10.1111/j.1365-2486.2009.02037.x, 2010.

Schubert, P., Eklundh, L., Lund, M., and Nilsson, M.: Estimating northern peatland CO 2 exchange from MODIS time series data, Remote Sensing of Environment, 114, 1178-1189, 2010.

Seidl, R., Schelhaas, M. J., Rammer, W., and Verkerk, P. J.: Increasing forest disturbances in Europe and their impact on carbon storage (vol 4, pg 806, 2014), Nat. Clim. Chang., 4, 930-930, 10.1038/nclimate2393, 2014.

Sellers, P.: Canopy reflectance, photosynthesis, and transpiration, II. The role of biophysics in the linearity of their interdependence, Remote sensing of Environment, 21, 143-183, 1987.

Senn, J., Hanhimäki, S., and Haukioja, E.: Among-Tree Variation in Leaf Phenology and Morphology and Its Correlation with Insect Performance in the Mountain Birch, Oikos, 63, 215-222, 10.2307/3545381, 1992.

Sonesson, M., and Lundberg, B.: Late Quaternary Forest Development of the Torneträsk Area, North Sweden. 1. Structure of Modern Forest Ecosystems, Oikos, 25, 121-133, 10.2307/3543633, 1974.

Tenow, O.: The outbreaks of Oporinia autumnata Bkh. & Operophtera spp. (Lep., Geometridae) in the Scandinavian mountain chain and northern Finland 1862–1968. Zoologiska Bidrag Från Uppsala, Supplement 2, 1972.

Tenow, O.: Hazards to a Mountain Birch Forest: Abisko in Perspective, Ecological Bulletins, 104-114, 1996.

Tenow, O., and Bylund, H.: Recovery of a Betula pubescens Forest in Northern Sweden after Severe Defoliation by Epirrita autumnata, Journal of Vegetation Science, 11, 855-862, 2000.

Tenow, O., Nilssen, A. C., Bylund, H., and Hogstad, O.: Waves and synchrony in Epirrita autumnata /Operophtera brumata outbreaks. I. Lagged synchrony: regionally, locally and among species, Journal of Animal Ecology, 76, 258-268, 10.1111/j.1365-2656.2006.01204.x, 2007.

Tømmervik, H., Høgda, K. A., and Karlsen, S. R.: in: Nordic mountain birch ecosystems, edited by: Wielgolaski, F. E., The Parthenon Publishing Group., London, 241-249, 2001.

Tucker, C. J.: Red and photographic infrared linear combinations for monitoring vegetation, Remote Sensing of Environment, 8, 127-150, 1979.

Turner, D. P., Urbanski, S., Bremer, D., Wofsy, S. C., Meyers, T., Gower, S. T., and Gregory, M.: A cross-biome comparison of daily light use efficiency for gross primary production, Global Change Biology, 9, 383-395, 2003.

Vanhanen, H., Veteli, T., Päivinen, S., Kellomäki, S., and Niemelä, P.: Climate change and range shifts in two insect defoliators: gypsy moth and nun moth – a model study, 4, 2007.

Wielgolaski, F.E.: Vegetation sections in northern Fennoscandian mountain birch forests. In F.E. Wielgolaski (Ed.), Nordic Mountain Birch Ecosystem. (pp. 23–46). London: The Parthenon Publishing Group, 2001.

Wu, C., Munger, J. W., Niu, Z., and Kuang, D.: Comparison of multiple models for estimating gross primary production using MODIS and eddy covariance data in Harvard Forest, Remote Sensing of Environment, 114, 2925-2939, http://dx.doi.org/10.1016/j.rse.2010.07.012, 2010.

Wulder, M. A., Dymond, C. C., White, J. C., Leckie, D. G., and Carroll, A. L.: Surveying mountain pine beetle damage of forests: A review of remote sensing opportunities, Forest Ecology and Management, 221, 27-41, DOI: 10.1016/j.foreco.2005.09.021, 2006.

Xiao, X., Zhang, Q., Braswell, B., Urbanski, S., Boles, S., Wofsy, S., Moore Iii, B., and Ojima, D.: Modeling gross primary production of temperate deciduous broadleaf forest using satellite images and climate data, Remote Sensing of Environment, 91, 256-270, http://dx.doi.org/10.1016/j.rse.2004.03.010, 2004.